Supplementary Information for

In Situ (S)TEM Investigation of Phase Transformation Mechanism in $LiNiO_2$ Cathode During Cycling

Ioannis Siachos[1,2], Xiaodong Liu[1], Weiqun Li[1,2], Amirafshar Moshtaghpour[1,3], Annalena R. Genreith-Schriever[2,4], Tingting Yang[5], Penghan Lu[5], Rafal E. Dunin-Borkowski[5], Clare P. Grey[2,4], B. Layla Mehdi[1,2]

[1] Department of Mechanical, Materials and Aerospace Engineering, University of Liverpool, Liverpool, L69 3GH, United Kingdom.

[2] The Faraday Institution, Harwell Campus, Didcot, OX11 0RA, United Kingdom.

[3] Correlated Imaging Group, Rosalind Franklin Institute, Harwell Science and Innovation Campus, OX11 0QS, United Kingdom.

[4] Department of Chemistry, University of Cambridge, Cambridge, CB2 1EW, United Kingdom.

[5] Ernst Ruska-Centre for Microscopy and Spectroscopy with Electrons, Research Centre Juelich, 52425 Juelich, Germany.

1. SEM Imaging of LNO cathode

Scanning Electron Microscopy (SEM) images of the pre- pared LNO powder are illustrated in Fig. S1, where secondary CAM particles are shown at the micro scale, with the expected spherical shape and the typical hierarchical structure. Fig. S1b, and the inset image, illustrates that the secondary particles consist of densely packed primary particles of 100–250 nm diameter, which explains the relatively small Brunauer-Emmett-Teller surface area of about 0.3 m^2g^{-1} measured for this material.

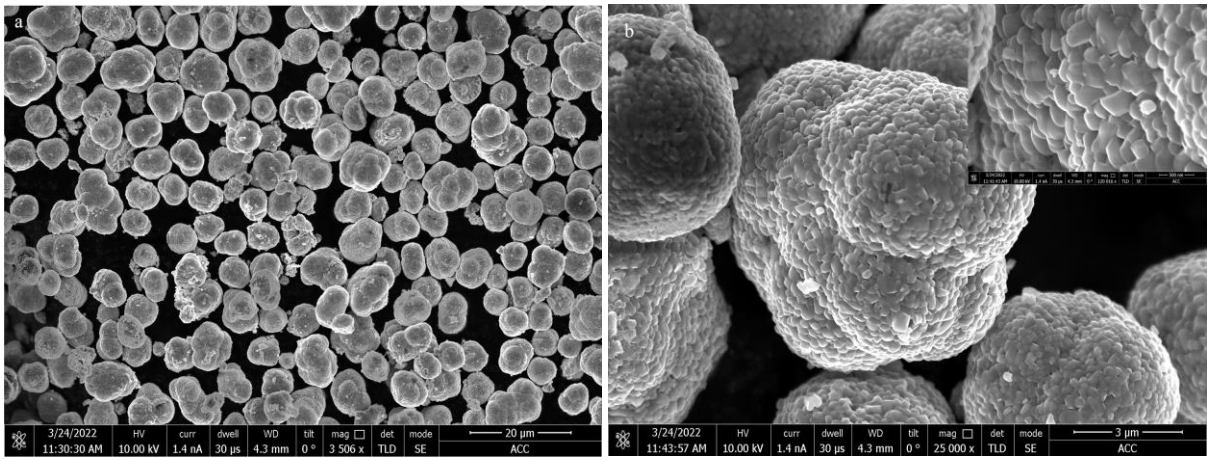

Figure S1: SEM figures of LNO cathode particles at different magnifications. The secondary particle nature of the material is visible, and an inset OF (b) shows the surface texture in detail.

2. EDS Analysis

Energy-dispersive X-ray spectroscopy (EDS) was used to characterize the compositional distribution of the LNO nanoparticles. The EDS mappings in Fig. S2 show the distribution of the main elements Ni, and O at the pristine state Fig. S2c,d. Signals from carbon and copper come from the holey carbon Cu grid and silicon from the EDS detector ring.

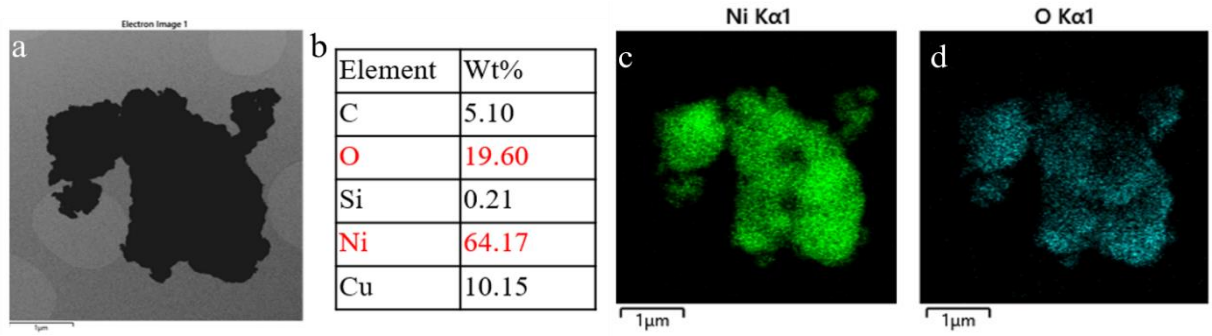

Element	Wt%
C	5.10
O	19.60
Si	0.21
Ni	64.17
Cu	10.15

Figure S2: EDS mapping shows a) the electron image of LNO particle, b) elemental composition presented as the wt% of the main elements Ni, O, and other elements appeared from the experimental set-up, c) map of Nickel in green colour suggesting that is the main element of the structure and d) map of Oxygen.

3. *Ex situ* TEM Characterization

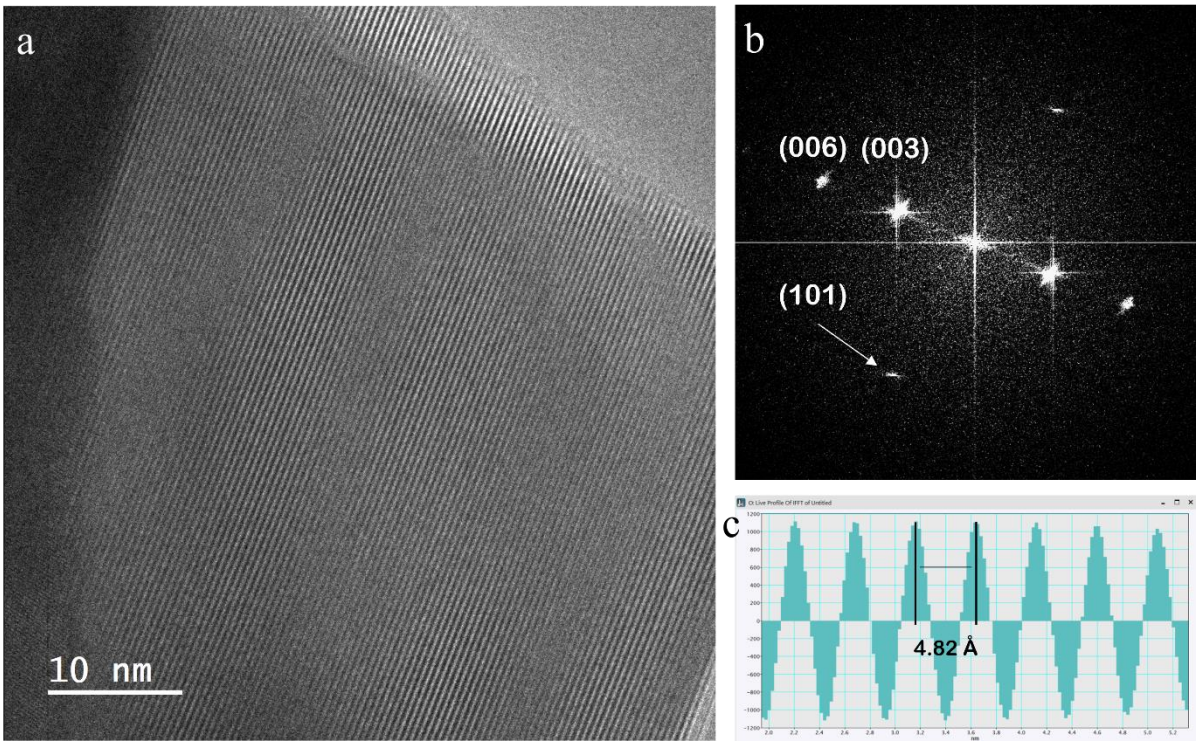

Figure S3: (a) High-resolution TEM image illustrates clearly the layered structure of the pristine LNO with distinct atomic planes of the (003) facet. (b) Selected area diffraction pattern of TEM image showing the main reflections. The line profile is used to calculate the d-spacing of that facet, which is 4.8 ˚A (c).

4. Control experiment: Li/Li_2O–LNO contact without applied bias

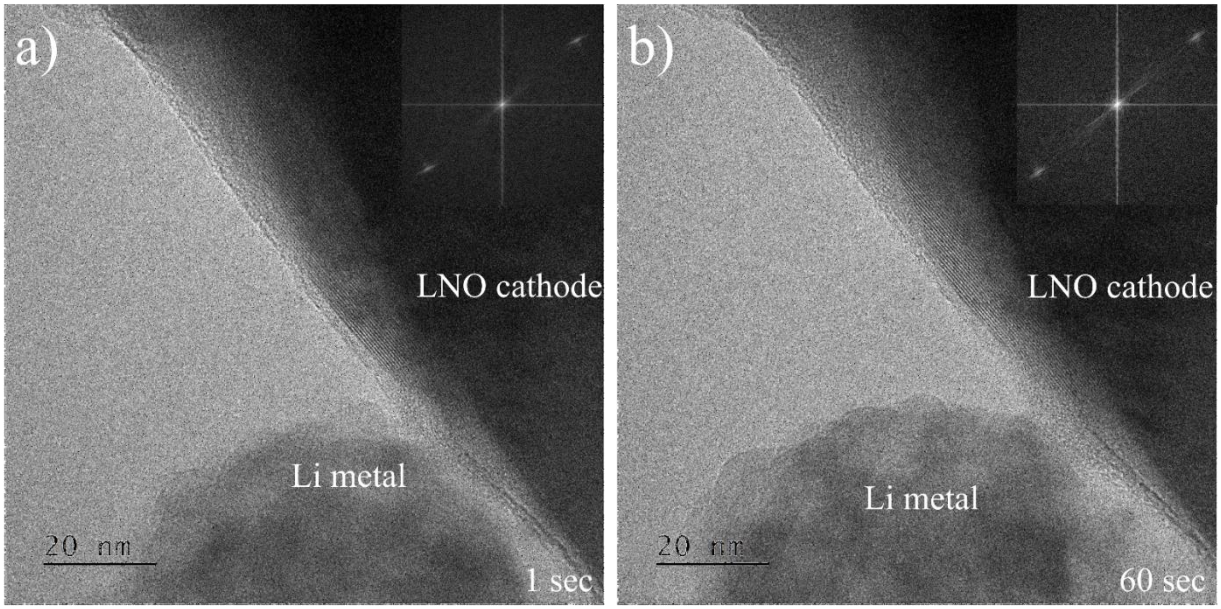

Figure S4: (a,b) Time-resolved TEM images of an LNO particle brought into direct physical contact with Li/Li_2O without applied electrical bias, acquired at 1 s and 60 s, respectively. FFTs (insets) confirm preservation of the layered structure with intact (003) reflections. No lattice expansion, phase transition, crystallinity loss, or rock-salt formation is observed. This control demonstrates that neither physical contact nor electron-beam exposure alone induces the transformations reported under applied bias.

5. EELS Spectrums

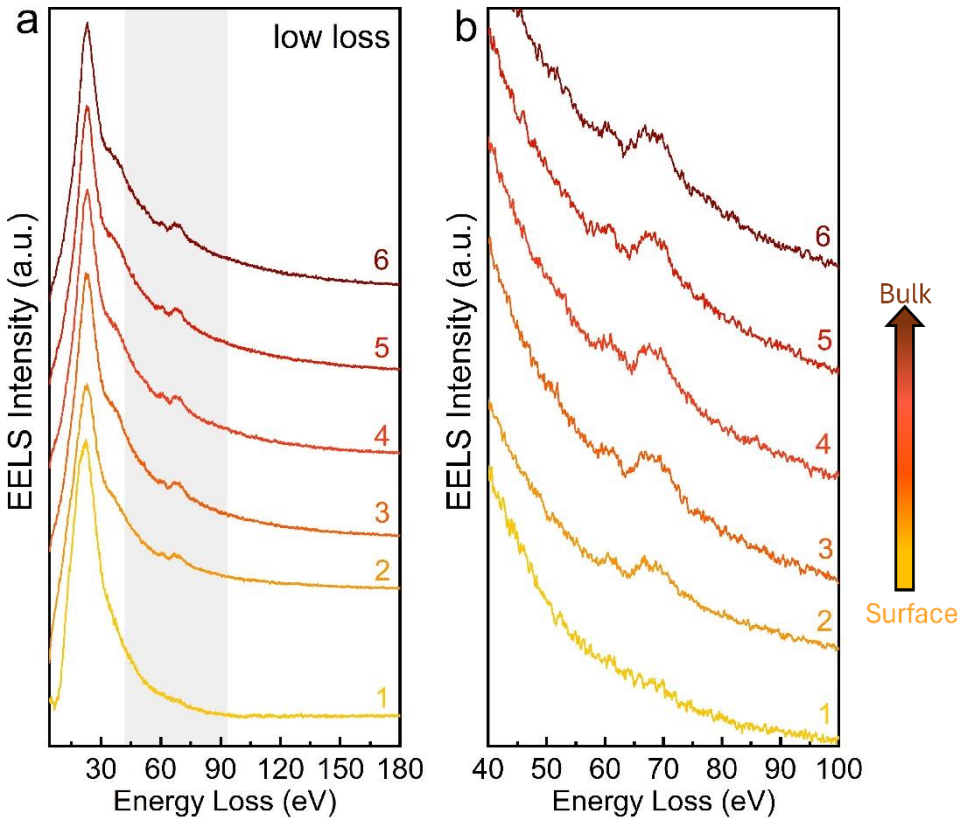

Figure S5: EELS spectrum taken at the low loss region of $LiNiO_2$, close to the zero-loss peak. 6 spectrums taken within the LNO particle (fig.5). 1 is taken from the surface, 6 from the bulk.

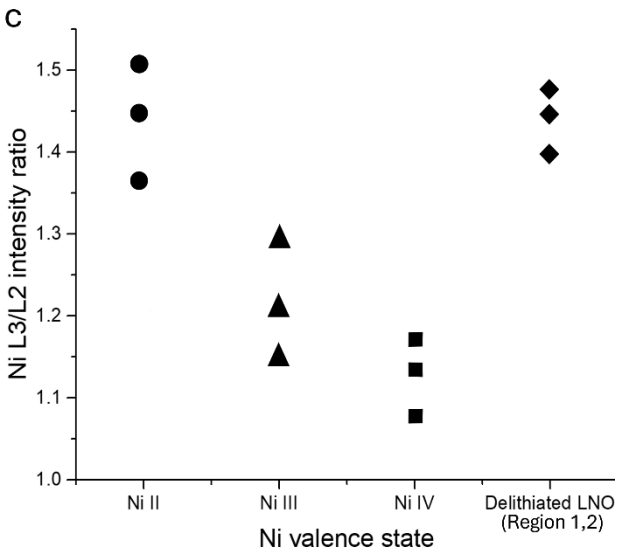

Figure S6: Ni L3/L2 intensity of ratio as calculated between three reference samples (NiO for Ni II, LNO for Ni III, and Ni peroxide for Ni IV) and one experimental spectrum taken from the reaction front (red-pink region) of the particle.

6. Electron dose during in situ TEM and EELS experiments

To minimize electron-beam–induced damage during STEM/EELS, all measurements were performed on native $LiNiO_2$ particles mounted on the edge of a holey carbon Cu grid, avoiding FIB preparation and Ga contamination. EELS spectra were acquired only from relatively thin edge regions of the particles. STEM/EELS was conducted at 200 kV using a convergence angle of 8.3 mrad, a probe current of ~10 pA, and dwell times of 2–3 ms per pixel. Single-pass line scans were used exclusively, without repeated exposure of the same region. These conditions correspond to an estimated electron dose rate of ~10^2–10^3 $e^-/Å^2s$.

All *in situ* TEM videos and operando observations reported in the main text were acquired under low-dose imaging conditions, with an estimated electron dose rate of ~50 $e^-/Å^2s$. Under these conditions, voltage-driven delithiation of $LiNiO_2$ (LNO) resulted in rapid, directional phase transformations, including lattice expansion, Ni/Li disordering, oxygen-hole depletion, and rock-salt formation. The control experiment as presented in Figure S4 was performed at a slightly higher dose rate of ~90 $e^-/Å^2s$.

7. *In situ* TEM Movies of LNO Delithiation

Movie S1. Low magnification video of the reaction between Li tip and LNO during Li removal when positive voltage is applied. 70 seconds of delithiation led to 26% expansion of the LNO particle.

Movie S2. Low magnification video of the reaction between Li^+/Li_2O and LNO during lithium de-intercalation, when positive voltage is applied (4.3V). 60 seconds of delithiation led to 30.6% expansion of the LNO particle.

Movie S3. HRTEM video shows the reaction between LNO and Li tip when +4.3V is stored in the battery cathode. The movie shows the phase transition of the (003) atomic planes of LNO into rocksalt (NiO) upon delithiation.

Movie S4. HRTEM video showing the dynamic reactions that take place within the LNO particle during Li ions removal process